MOLECULAR AND CELLULAR BIOLOGY, Aug. 2007, p. 5393–5402 Vol. 27, No. 15
0270-7306/07/$08.00+0 doi:10.1128/MCB.00288-07

Splicing Regulator SC35 Is Essential for Genomic Stability and Cell Proliferation during Mammalian Organogenesis[▽]

Ran Xiao,[1,2]† Ye Sun,[1]† Jian-Hua Ding,[2]† Shengrong Lin,[2,3]† Dave W. Rose,[4] Michael G. Rosenfeld,[4,5] Xiang-Dong Fu,[2]* and Xue Li[1]*

Department of Surgery/Urology and Department of Pathology, Children's Hospital of Boston, Harvard Medical School, 300 Longwood Ave., Boston, Massachusetts 02115[1]; Department of Cellular and Molecular Medicine, University of California, San Diego, 9500 Gilman Dr., La Jolla, California 92093[2]; and Department of Pathology,[3] Department of Medicine,[4] and Howard Hughes Medical Institute,[5] University of California, San Diego, 9500 Gilman Dr., La Jolla, California 92093

Received 16 February 2007/Returned for modification 30 March 2007/Accepted 15 May 2007

The members of the SR family of splicing regulators were initially characterized for their critical roles in constitutive and regulated splicing. They are implicated in different aspects of gene expression processes, including transcription, RNA stability, mRNA transport, and translational control. While knockout studies have demonstrated their essential functions during animal development, the pathway(s) leading to a specific cellular phenotype remains poorly understood. We report here that the SR protein SC35 controls cell proliferation during pituitary gland development but is completely dispensable in terminal differentiated mature cardiomyocytes in mice. We show that loss of *SC35* in mouse embryonic fibroblasts induces G_2/M cell cycle arrest and genomic instability, resulting at least in part from p53 hyperphosphorylation and hyperacetylation. While p53 hyperphosphorylation appears related to ATM activation, its hyperacetylation has been attributed to the increased expression of the acetyltransferase gene *p300* and the aberrant splicing of the deacetylase gene *SirT1*. These findings reveal the involvement of SC35 in specific pathways in regulating cell proliferation and genomic stability during mammalian organogenesis and suggest its potential function in tumorigenesis.

More than half of the protein-coding genes undergo alternative splicing in humans, suggesting that regulated splicing plays a fundamental role in cellular physiology and organ development (5). In addition, pre-mRNA splicing is not only an essential intermediate step in gene expression but also connects upstream transcriptional events and downstream mRNA export, degradation, and even translation (20). Given the importance of pre-mRNA splicing in gene expression and in various developmental and disease processes (12), we are still at the beginning of understanding the roles of distinct splicing regulators in cell proliferation and cell cycle progression that lead to specific cellular and developmental phenotypes.

The present study focuses on the role of the SR family of splicing regulators. SR proteins are a family of RNA binding proteins characterized by one or two RNA recognition motifs and a signature RS domain enriched with arginine and serine repeats, hence the name for this family. SR proteins play critical roles in both constitutive and alternative splicing (14, 17, 31, 35). It is generally assumed that they play important housekeeping roles in most, if not all, cell types. Indeed, knockout of individual SR genes in mice resulted in early embryonic lethality (21, 46, 48). Similarly, in experiments using chicken DT40 cells or mouse embryo fibroblasts (MEFs) derived from conditional knockout embryos, ablation of SR protein ASF/SF2 gave rise to a cell-lethal phenotype (32, 47). In the case of DT40 cells, cell mortality induced by ASF/SF2 depletion appears to be caused by multiple defects, including genomic instability triggered by elevated double-strand DNA break and subsequent apoptosis (26, 27, 29).

Here, on the basis of experiments using conditional mouse knockout and inducible somatic genetic complementation systems, we report that the SR protein SC35 plays a critical role in cell proliferation during pituitary development, but surprisingly it is dispensable in terminal differentiated mature cardiomyocytes in the heart. Using the conditional knockout MEF model, we found that depletion of SC35 induced cell cycle arrest at the G_2/M phase. Remarkably, such a defect in cell cycle progression could be partially relieved by inactivation of the *p53* tumor suppressor gene, indicating a key role of p53 in the SC35-mediated cell proliferation pathway. Analysis of the p53 activation mechanism revealed hyperphosphorylation of p53 at the site known to be modified by activated ATM (1), consistent with the double-stranded DNA break observed in SC35-deficient MEFs. We also detected p53 hyperacetylation, which was linked to the increased expression of the p53 acetyltransferase gene *p300* (4, 18, 23, 33, 39) and the aberrant splicing of the p53 deacetylase gene *SirT1* (2, 9, 34, 45). These observations provide evidence for a general role of SR proteins in maintaining genomic stability and cell proliferation in vertebrates. The ability of SR proteins to modulate p53 functions in cell growth control suggests a novel mechanism for overex-

* Corresponding author. Mailing address for Xue Li: Department of Surgery/Urology and Department of Pathology, Children's Hospital of Boston, Harvard Medical School, 300 Longwood Ave., Boston, MA 02115. Phone: (617) 919-2703. Fax: (617) 730-0530. E-mail: sean.li@childrens.harvard.edu. Mailing address for Xiang-Dong Fu: Department of Cellular and Molecular Medicine, University of California, San Diego, 9500 Gilman Dr., La Jolla, CA 92093. Phone: (858) 534-4937. Fax: (858) 822-6920. E-mail: xdfu@ucsd.edu.
† These authors contributed equally to this work.
▽ Published ahead of print on 25 May 2007.

pressed SR proteins detected in various tumor types (13, 16, 43) to contribute to cancer progression.

MATERIALS AND METHODS

Generation of *Pit-Cre/AP* transgenic mice. Standard molecular biology procedures were used to generate the *Pit-Cre/hpAP* transgene construct. In brief, the 15.5-kb endogenous *Pit-1* promoter and enhancer region was cloned in front of the mini-β-globin intron region and the full-length Cre cDNA, which was followed by human placenta alkaline phosphatase (hpAP) and a poly(A^+) signal. The hpAP cDNA is fused with internal ribosomal entrance sites, which allows Cap-independent translation (25, 30). The transgenic mice were generated by direct injection of fertilized eggs with the linearized transgene construct.

AP and β-galactosidase staining. Transgene expression was analyzed by monitoring the hpAP enzymatic activity as described previously (25, 30). In brief, staged embryos were dissected and fixed in 10% buffered formalin at 4°C for 30 min. The cryosections from each embryo were postfixed for 30 min and rinsed with phosphate-buffered saline (PBS) twice before heat inactivation of endogenous AP activity (25). The hpAP activity was then assayed at room temperature overnight using BM purple substrate from Roche. The Cre recombinase function was analyzed by crossing the transgenic mice with the ROSA26 reporter mice, followed by 5-bromo-4-chloro-3-indolyl-β-D-galactopyranoside staining for β-galactosidase activity, essentially by the method described previously (42).

Ablation of *SC35* in the pituitary and heart. The conditional *SC35* knockout allele was generated by flanking both axons of the entire *SC35* locus with two *loxP* sites as described previously (46). Homozygous type II *SC35* mice were crossed with the *Pit-Cre/hpAP* transgenic mice to generate pituitary-specific deletion of the *SC35* gene. To ablate *SC35* in the adult heart, the conditional *SC35* knockout mice were similarly crossed to the tamoxifen-inducible *MHC-Cre* transgenic mice (41). To induce gene deletion, tamoxifen was intraperitoneally injected into 3-week-old mice once a day for 5 days, as described previously (41). Deletion efficiency was determined by Southern blot analysis, and echocardiographic analysis was performed as previously described (11).

Cell type determination by immunohistochemistry, BrdU labeling, and TUNEL assays. All pituitary-specific antibodies and the immunohistochemistry procedure used were described previously (28). 5-Bromo-2-deoxyuridine (BrdU) labeling and terminal deoxynucleotidyltransferase-mediated dUTP-biotin nick end labeling (TUNEL) assay were performed according to the manufacturer's suggestions and as described previously (28). Briefly, staged pregnant females and newborn pups were labeled for 2 h with BrdU-PBS at 0.1 mg/g of body weight. Incorporated BrdU was detected on 10-μm cryostat sections as recommended by the manufacturer (ICN, Irvine, CA). All sections were counterstained with 4′,6′-diamidino-2-phenylindole (DAPI) before being photographed.

Plasmids, Tet-off-inducible system, and TAT-Cre protein transduction. The pRevTRE-SC35 plasmid was constructed by subcloning hemagglutinin (HA)-tagged SC35 cDNA into the pRevTRE vector (Clontech), which was used to produce a retrovirus. T-antigen-immortalized MEFs carrying floxed SC35 alleles were coinfected with RevTRE-SC35 and RevTet-OFF-IN viruses, followed by single-cell cloning and removal of the endogenous *SC35* gene to establish the inducible *SC35* expression cell line as described for ASF/SF2 (32). The SC35 Tet-off cell line was verified by PCR genotyping (primers used were F, 5′AAA ATG TCT TGC CAT CTC CCT CCC C3′; R1, 5′GGT CTT GGT TAT TTG GCC AAG AAT CAC3′; and R2, 5′TCC ATG GAC CGA TGG ACT GAG TTT GT3′; the PCR conditions were 35 cycles of 94°C for 30 s, 65°C for 30 s, and 72°C for 60 s) and characterized by Western blotting. Complementation was carried out using wild-type (wt) and mutant SC35 expressed as a Myc-tagged fusion protein from the retrovirus.

Cell proliferation and cell cycle analyses. Cells were cultured in 12-well plates. The culture medium was changed 24 h before the MTT [3-(4,5-dimethylthiazol-2-yl)-2,5-diphenyltetrazolium bromide] assay; 100 μl of MTT stock solution (5 mg/ml in PBS) was added to each well, which contained 1.0 ml of medium, and the plate was incubated at 37°C for 1 h. After the medium was removed, the converted dye was solubilized with 1 ml of acidic isopropanol (0.04 M HCl in absolute isopropanol) and, within 1 h after the addition of isopropanol, the reaction in a 12-well plate was measured at 570 nm with a background subtraction at 670 nm. BrdU uptake studies were also performed using an in situ cell proliferation kit (Roche). The short interfering RNA (siRNA) microinjection assay was essentially the same as that previously described (37).

To profile the cell cycle in *SC35*-depleted MEFs, doxycycline (Dox) was included in the media for 5 days. Induced cells and similarly treated wt controls were harvested, washed with PBS, and fixed in 70% ethanol–PBS for 30 min at 4°C. Cells were washed with PBS and stained with propidium iodide solution for 30 min at room temperature in the dark before fluorescence-activated cell sorter (FACS) analysis on an LSR flow cytometer (Becton Dickinson).

Western blotting and immunofluorescence staining. Whole-cell protein was extracted in sodium dodecyl sulfate loading buffer for polyacrylamide gel electrophoresis. After being blotted onto nitrocellulose, the membrane was probed with anti-αHA (Roche). To detect p53 modifications, the cells were lysed in a Flag lysis buffer (34) and were analyzed by Western blotting using anti-total p53 (FL-393; Santa Cruz Biotechnology), anti-phospho-p53 serine 18 (16G8; Cell Signaling), and anti-acetyl-p53K379 and anti-acetyl-p53K317 (2271-PC-050; Trevigen). Anti-SirT1 was from Upstate (07-131).

For immunofluorescence staining, cells were fixed with 4% paraformaldehyde in PBS for 20 min at room temperature and permeabilized in 0.5% Triton X-100 for 5 min. The fixed cells were incubated for 1 h at room temperature with anti-phospho-histone γH2AX-ser139 (2F3; Biolegend) in PBS plus 1% fetal bovine serum. After being washed, the cells were developed for 1 h at room temperature with Alexa Fluor 594-conjugated donkey anti-mouse immunoglobulin G (1:500; Molecular Probes) and Alexa Fluor 488-conjugated phalloidin (1:500; Molecular Probes). Coverslips were mounted with a mounting solution containing DAPI and were imaged with a Zeiss Axioskop microscope.

RESULTS

Reduced pituitary gland cell proliferation in SC35 conditional knockout mice. To understand the specific function of SC35 during mammalian development, we genetically engineered tissue-specific SC35 ablation in the well-characterized anterior pituitary gland primordium at embryonic day 9.5 (e9.5) with the *Pitx/Cre* transgenic mouse (37). Histological analyses revealed growth arrest of the anterior pituitary gland at e10.5 and e15.5, but the *Cre* expression-negative posterior pituitary gland was unaffected (Fig. 1A and data not shown). This result demonstrates the essential role of SC35 in pituitary development, but the severe anterior pituitary gland growth arrest phenotype precluded further analysis of SC35 function during pituitary cell differentiation and proliferation at later developmental stages. We therefore generated another transgenic line, *Pit-1-Cre/hpAP*, to express the Cre recombinase at later pituitary development stages, starting at e13.5, using a 15.5-kb *Pit-1* promoter. This promoter contains all the regulatory information of the *Pit-1* gene and is capable of driving specific transgene expression in all three *Pit-1* cell lineages: the somatotrophs, lactotrophs, and thyrotrophs (Fig. 1B) (10, 38). The dicistronic transgene expresses both the Cre recombinase and a separate hpAP by using an internal ribosomal entrance site (Fig. 1B) (25). The spatiotemporal expression pattern of the transgene was analyzed initially based on the hpAP enzymatic activity, demonstrating the early transgene activity at e13.5 that coincided with the initial expression of the endogenous *Pit-1* gene and the onset of the pituitary gland cell type differentiation (Fig. 1C). Immunohistochemical analysis using a Pit-1-specific antibody on the adjacent section showed that the hpAP activity colocalized with the *Pit-1* expression pattern (Fig. 1C), and strong transgene expression persisted in the adult pituitary (Fig. 1D). The enzymatic activity of Cre was further confirmed on the basis of the expression of β-galactosidase using the ROSA26 Cre reporter mice (data not shown) (42).

Conditional deletion of *SC35* using *Pit-1-Cre/hpAP* transgenic mice produced apparently normal adult mice according to their Mendelian frequency, and the mutant mice exhibited body weights comparable to those of wt littermate controls (data not shown). Gross analyses of the pituitary gland, however, revealed that the *SC35*-deficient gland was only 1/5 to 1/10 the size of those of wt littermate controls (Fig. 1D). A

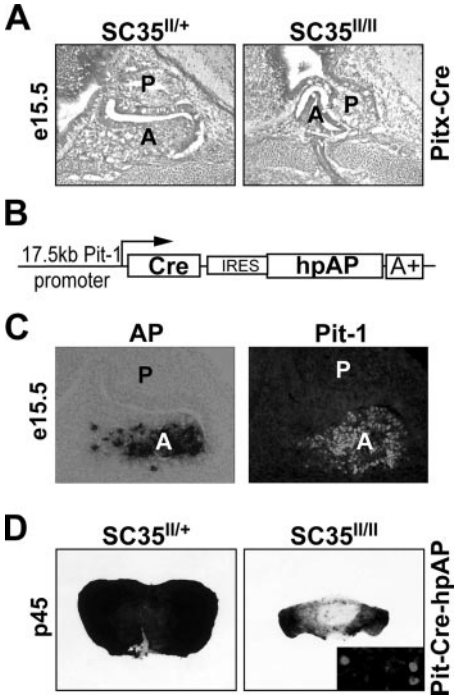

FIG. 1. Pituitary agenesis in *SC35* conditional knockout mice. (A) Early deletion of *SC35* by the *Pitx/Cre* transgene resulted in severe anterior pituitary gland (labeled "A") agenesis. The Cre-negative posterior pituitary gland (labeled "P") is not affected. (B) Schematic diagram of the *Pit-1-Cre/hpAP* dicistronic transgene. IRES, internal ribosome entrance site. (C) Expression of the transgene (AP staining) and Pit-1 protein (immunostaining) on adjacent sections of a pituitary gland from the transgenic mouse. (D) AP staining revealed hypoplastic adult pituitary glands in *SC35* conditional knockouts. The insert shows Cre immunoactivity.

small population of Cre-positive cells persisted in the mutant pituitary gland on the basis of the positive AP enzymatic activity (Fig. 1C) and Cre immunoactivity (Fig. 1D, inset). The severe hypolastic pituitary phenotype potentially could be due to defects in *Pit-1* cell lineages, including increased cell death, reduced cell proliferation, and/or lack of cell differentiation. Because loss of SR proteins has been shown to induce apoptosis in DT40 cells (29), we examined potential increases in programmed cell death in the mutant pituitary gland by using a TUNEL assay. We could not detect any significant increase in the number of apoptotic cells in the mutant pituitary gland either during embryonic stages (e13.5, e14.5, e15.5, and e17.5) or during postnatal stages (postnatal day 2 [p2], p8, p15, p21, p28, and p35) (data not shown). These results indicate that cell death may not account for the severe hypoplastic phenotype caused by *SC35* deletion.

We next determined whether *SC35* ablation could prevent cell differentiation. Each cell type in the *Pit-1* lineage expresses a distinct terminal hormonal marker (e.g., growth hormone [GH] from somatotrophs, prolactin from lactotrophs, and β-unit thyroid-stimulating hormone from thyrotrophs). A small population of terminal differentiated *Pit-1*-dependent cell lineages was clearly detectable on the basis of immunohistochemical analysis of the mutant adult pituitary gland (Fig. 2A and data not shown). In contrast, the *Pit-1*-independent gonadotrophs (luteinizing hormone [LH] positive) and corticotrophs (adrenocorticotropic hormone [ACTH] positive) were not affected (Fig. 2A). The increased density of LH-positive and ACTH-positive cells likely was due to the reduction of the *Pit-1*-lineage cells, and as a result, those non-*Pit-1*-lineage cells became dominant cell populations in SC35-deficient pituitary glands. Alpha glycoprotein hormone subunit (αGSU) is a common α-glycoprotein specifically expressed in both gonadotropes (LH and follicle-stimulating hormone positive) and thyrotropes (thyroid-stimulating hormone positive). In the SC35 conditional deletion embryos of *Pit1-Cre/hpAP* mice, the numbers of thyrotropes are significantly reduced. However, gonadotropes are not affected. Therefore, the overall density of αGSU-positive cells seems to be increased, similar to what was seen with the LH staining pattern. The presence of GH-secreting somatotrophs is consistent with the observation that the mutant mice had normal body weights. To ascertain that the remaining *Pit-1*-lineage cells were indeed Cre positive, we examined the expression of the transgene in mutant mice and found high levels of hpAP activity in the adult pituitary (Fig. 1D and data not shown), ruling out the possibility that the survival of the remaining population of the *Pit-1*-lineage cells was a result of selective expansion of *Cre*-negative cells.

The results described above suggest the possibility that SC35 is required for cell proliferation. The pituitary precursor cells undergo rapid proliferation between e9.5 and e13.5 in developing embryos. The second wave of pituitary cell proliferation begins after birth. The proliferating cells were labeled with a thymidine base analog, BrdU, which is selectively incorporated into DNA during the S phase of the cell cycle. After 2 h of labeling, pituitary histological sections were prepared and analyzed for their BrdU incorporation rate. The mutant pituitary precursor cells had a proliferation rate that was very similar to that of wt littermate controls between e13.5 and e17.5 (data not shown), which is consistent with the fact that few *Pit1*-expressing cells proliferate during these embryonic stages. In contrast, the BrdU incorporation rate was significantly reduced in *SC35* mutant mice at p5 (~41% reduction), p11 (~50% reduction), and p28 (~58% reduction) (Fig. 2B). Together, these results provide definitive evidence for the requirement of SC35 in cell proliferation during pituitary organogenesis.

SC35 is dispensable in terminal differentiated mature cardiomyocytes. The requirement for SR splicing factors in cell proliferation may result from specific defects in cell growth pathways or from some general activities for cell survival. To distinguish between these possibilities, and more importantly, to closely examine the SC35 requirement in postmitotic cells, we chose to delete *SC35* in terminal differentiated mature cardiomyocytes by using a tamoxifen-inducible gene targeting strategy (41). We previously showed that conditional knockout of *SC35* during early cardiogenesis in mice resulted in severe cardiac hypertrophy (11). However, it remains to be determined whether the disease phenotype is due to developmental problems during cardiomyocyte differentiation/maturation or to cell-autonomous defects in mature cardiomyocytes. In this study, we crossed the conditional *SC35* knockout mouse with the transgenic mouse in which the expression of Cre was driven by the cardiomyocyte-specific myosin heavy-chain promoter in a tamoxifen-inducible fashion (41). By administration of tamoxifen at the postnatal stage of 3 weeks, *SC35* deletion was induced in adults with an efficiency comparable to that of

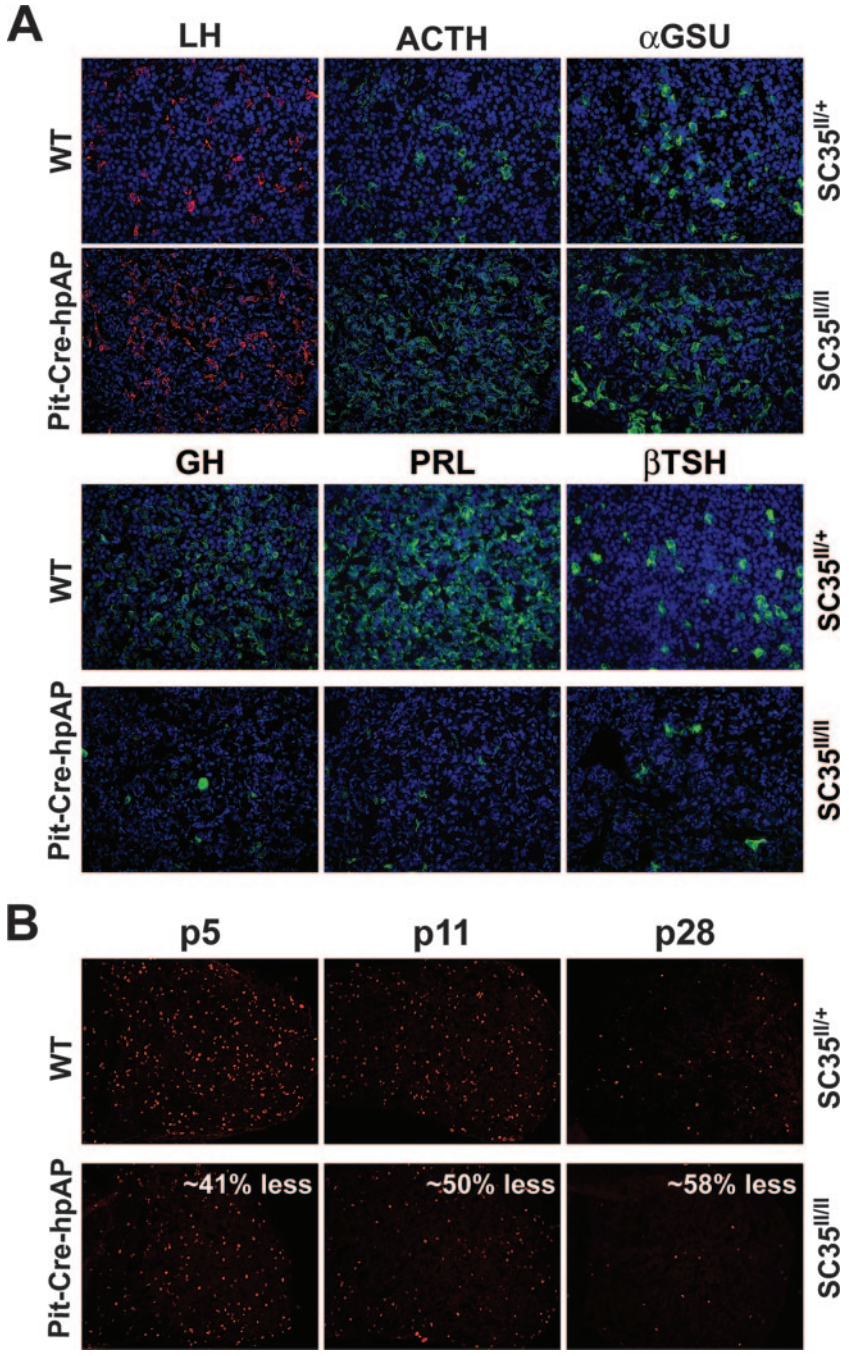

FIG. 2. SC35 is required for pituitary cell proliferation but not cell differentiation. (A) Immunohistochemical staining of adult pituitary glands using cell type-specific hormonal markers. The *Pit-1*-dependent lineages, somatotrophs (GH), lactotrophs (prolactin [PRL]), and thyrotrophs (β-unit thyroid-stimulating hormone [β-TSH]), were markedly reduced. The *Pit-1*-independent lineages, gonadotrophs (LH) and corticotrophs (ACTH), were unaffected, which resulted in the apparent increase in levels of these *Pit-1*-independent cell lineages in SC35-deficient pituitary glands. αGSU is expressed in both thyrotrophs and gonadotrophs. (B) Reduced cell proliferation detected by BrdU immunohistochemical staining (red) in postnatal pituitary gland at days p5 (~41% reduction), p11 (~50% reduction), and p28 (~58% reduction).

MLC2v-Cre-mediated ablation in embryos (Fig. 3A) (11). Significantly, the SC35 mutant mice exhibited no difference in survival compared to that of wt littermate controls during the period of more than 80 weeks of observation (Fig. 3B). Histological analysis of hearts from 80-week-old mice detected no cardiac hypertrophy in the mutant animals (data not shown). Furthermore, echocardiographic analysis of *SC35*-deficient mice revealed no functional defects in heart performance compared to that of wt littermate controls (Fig. 3C). Using the same strategy, we induced deletion of another SR protein, ASF/SF2, in adult hearts and observed total mortality in 2 months (Fig. 3B), thus unequivocally demonstrating the differential require-

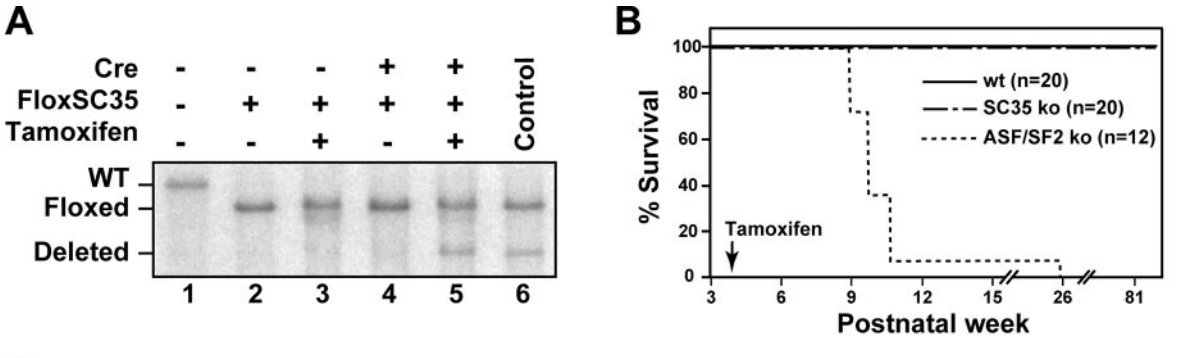

C

	Age (weeks)	HR (bpm)	IVSd (mm)	IVSs (mm)	LVPWd (mm)	LVPWs (mm)	LVEDd (mm)	LVEDs (mm)	%FS	VCF (circ/s)	HW (g)	BW (g)	HW/BW (%)
WT (n=5)	72 (± 2)	565 (± 37)	0.68 (± 0.04)	1.10 (± 0.10)	0.71 (0.03)	1.21 (± 0.11)	3.60 (± 0.47)	2.00 (± 0.39)	44.68 (± 7.56)	8.34 (± 1.59)	0.11 (± 0.02)	31 (± 7)	0.36 (± 0.03)
KO (n=5	72 (± 2)	519 (± 14)	0.70 (± 0.02)	1.15 (± 0.10)	0.71 (± 0.02)	1.29 (± 0.07)	3.53 (± 0.32)	1.89 (± 0.22)	46.34 (± 5.74)	8.32 (± 1.33)	0.12 (± 0.01)	36 (± 6)	0.36 (± 0.05)

HR: heart rate; IVSd: end-diastolic interventricular septum thickness; IVSs: end-systolic interventricular septum thickness; LVPWd: end-diastolic left ventricular posterial wall thickness; LVPWs: end-systolic LV posterial wall thickness; LVEDd: end-diastolic LV dimension; LVEDs: end-systolic LV dimension; %FS: fractional shortening; VCF: velocity of circumferential fiber shortening; HW: heart weight; BW: body weight;

FIG. 3. SC35 is not essential in terminal differentiated mature cardiomyocytes. (A) Genomic Southern blot analyses of tamoxifen-induced *SC35* deletion in adult hearts. Control DNA was from conditional *SC35* knockout (ko) mice mediated by MLC2v-Cre (11). (B) The Kaplan-Meier survival plot after tamoxifen-induced deletion of SC35 and ASF/SF2 in the adult heart. (C) Echocardiographic analysis of SC35-deficient mice. bpm, beats per minute; circ, circumferences.

ment for different SR proteins in the adult heart. We conclude that *SC35* is dispensable in mature postmitotic cardiomyocytes. These results are dramatically different from those for the developing heart (11) and pituitary (Fig. 1 and 2), suggesting that SC35 may play a specific role in the regulation of cell proliferation rather than providing a general function for cell survival.

SC35 plays a major role in cell cycle progress through the G_2/M phase in MEFs. We next studied SC35 function in cell proliferation by using the MEFs as a model. The type II conditional knockout MEFs ($SC35^{II/II}$) exhibited normal cell proliferation compared to that of wt MEFs (data not shown). To analyze the SC35 function in cell cycle progression, we took a somatic genetic strategy described earlier for creating conditional *ASF/SF2* knockout MEFs (32) by generating an *SC35*-null MEF line in which the endogenous *SC35* gene was deleted and the cell was complemented by exogenous, HA-tagged SC35 (HA-SC35) under an inducible Tet-off promoter (Fig. 4A). In the absence of Dox, the MEFs grew at a rate similar to

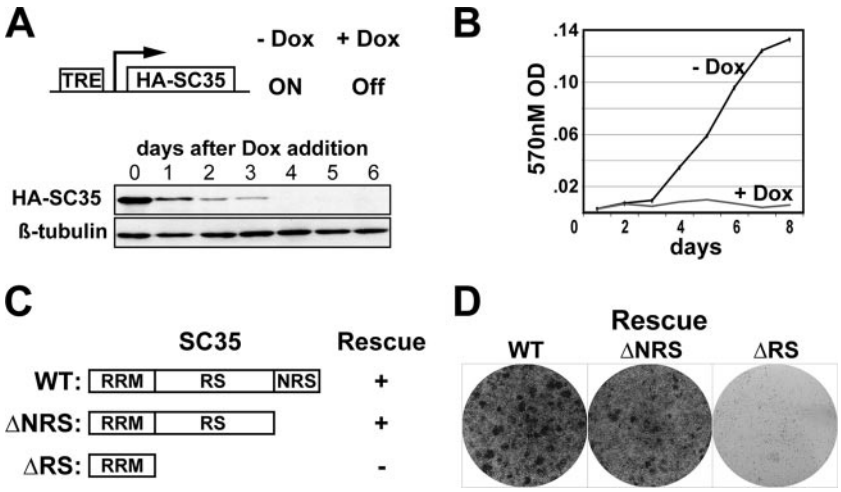

FIG. 4. Genetic complementation of *SC35* knockout MEFs. (A) Construction of a Tet-repressible SC35 expression unit and time course analyses of HA-SC35 expression after addition of Dox. TRE, Tet regulatory element. (B) Growth arrest induced by SC35 depletion in MEFs. (C and D) Functional rescue of SC35-depleted MEFs by wt and mutant SC35. 570 nM OD, optical density at 570 nm. RRM, recognition motif; RS, RS domain enriched with arginine (R) and serine (S) repeats; NRS, nuclear retention signal.

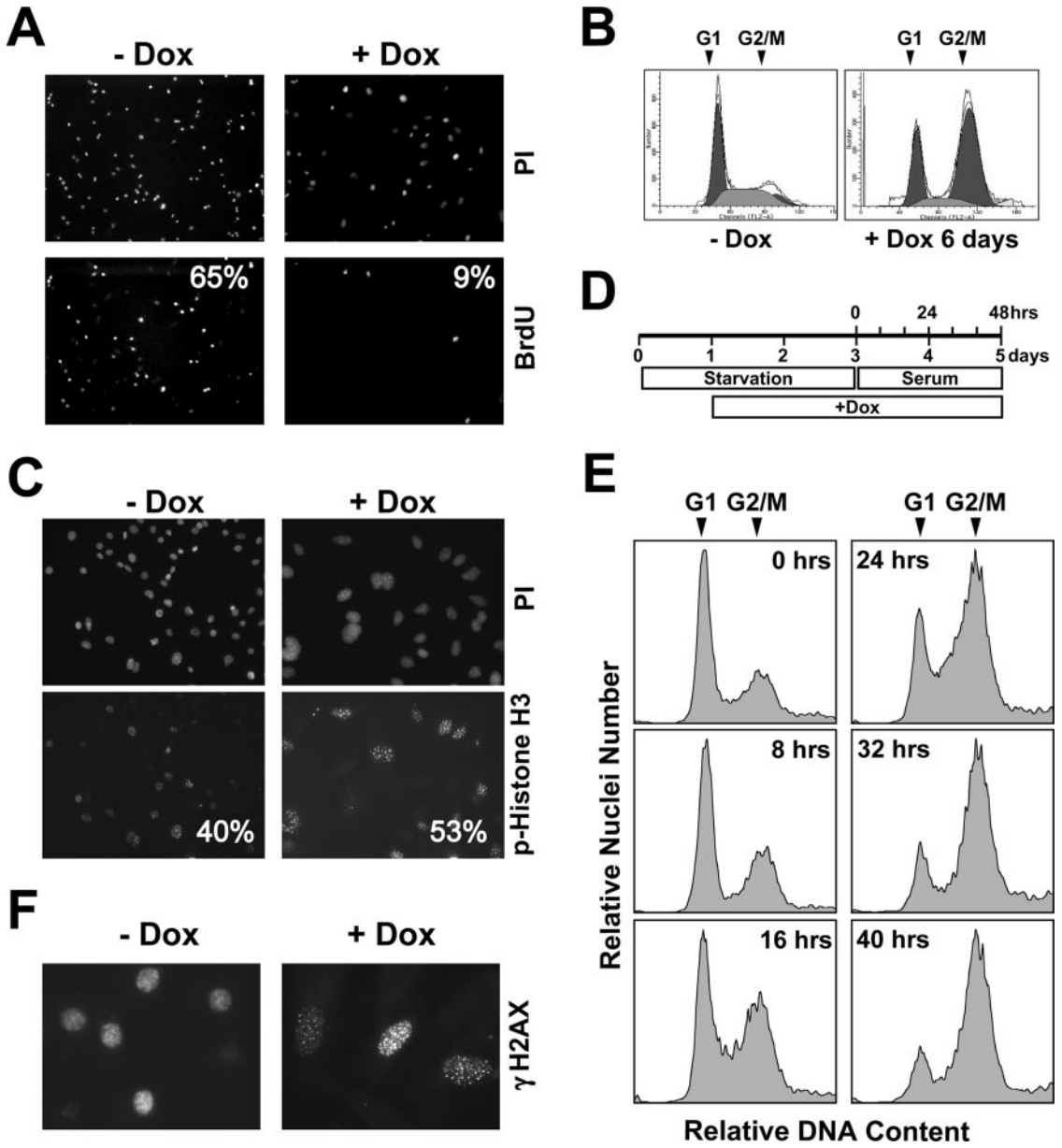

FIG. 5. G_2/M cell cycle arrest induced by *SC35* deficiency in MEFs. (A) Analysis of proliferating cells by BrdU labeling before and after SC35 depletion (5 days after Dox addition to the media). (B) FACS analysis of the cell cycle in wt and SC35-depleted MEFs (+Dox), showing a reduction in the number of S-phase cells and a dramatic increase in the number of G_2/M-phase cells. (C) Analysis of M-phase cells on the basis of staining for the mitotic phosphorylated histone H3 (p-Histone H3) marker (+Dox, 4 days). (D and E) Experimental design (D) and time course FACS analyses (E) of cell cycle progression of SC35-deficient MEFs (+Dox). (F) Immunocytochemical analyses of SC35-depleted cells (5 days after Dox treatment) by staining with an antibody against phosphorylated γH2AX to detect induced foci accumulated on broken DNA. PI, propidium iodide.

that of wt MEF controls (data not shown). Upon addition of Dox, levels of exogenous HA-SC35 diminished in 4 days (Fig. 4A), and cell proliferation was arrested almost instantly (Fig. 4B). *SC35*-depleted MEFs were rounded up in a week to 10 days and then died (data not shown). Analogous to the situation of the *SC35*-deficient pituitary, we did not detect any significant increase in apoptosis on the basis of both TUNEL assay and staining for annexin V and active caspase-3 (data not shown), indicating that programmed cell death was not a major event in MEFs, which is different from the situation for *ASF/SF2*-depleted chicken DT40 cells (24, 29). As expected, retroviral expression of wt full-length *SC35* completely rescued the proliferation defect in the presence of Dox (Fig. 4C and D). Interestingly, while the C-terminal nuclear retention signal (8) was dispensable, the RS domain was essential for SC35 to function in vivo (Fig. 4C and D), which is in contrast to the nonessential role of the RS domain of ASF/SF2 of MEFs (32).

Having established the somatic genetic complementation system for *SC35*, we next addressed its requirement in cell proliferation and cell cycle progression. By BrdU labeling, we found that the size of the S-phase cell population was dramatically reduced, from 65% to 9%, in the presence of Dox (Fig. 5A), suggesting a

major reduction in cell proliferation, as was as seen in the developing pituitary gland (Fig. 2B). The dramatic reduction in BrdU labeling suggests potential G_1/S cell cycle arrest triggered by the activation of the S-phase checkpoint in *SC35*-deficient MEFs. To examine this possibility, we determined the cell cycle profile and found that SC35 depletion induced G_2/M arrest (Fig. 5B). Furthermore, the M-phase cell population was increased from 40% to 53% on the basis of cell staining with an antibody against phosphorylated histone H3 at serine 10, a marker for mitotic cells, which was correlated with an overall increase in cell size (Fig. 5C and data not shown). These observations indicate that the reduction of S-phase cells is an indirect effect of cell cycle arrest at the G_2/M phase.

To directly demonstrate that the *SC35*-deficient MEFs can successfully progress through the S phase, we analyzed cell cycle progression by arresting the mutant cells at G_1 phase via serum starvation, followed by monitoring cell cycle progression by FACS after serum stimulation (Fig. 5D). One day after serum starvation, Dox was added to the culture to deplete SC35. After 3 days of serum starvation (Fig. 5D and E), cells were relatively arrested at the G_1 phase; upon serum addition, these cells were progressively transited through S phase, and the majority of cells were arrested at the G_2/M phase (Fig. 5E). These results suggest that the DNA replication machinery is competent in *SC35*-depleted MEFs and that SC35 may play a critical role in the regulation of the G_2/M cell cycle transition.

These observations are reminiscent of the phenotype observed for chicken DT40 cells, in which the cell cycle defect was attributed to double-strand DNA breaks induced by depletion of ASF/SF2 (26). To determine whether double-strand DNA breaks also take place in normal cells, such as MEFs, and are a general phenotype in response to in vivo depletion of SR proteins, we stained the cells with an antibody against phosphorylated histone γH2AX at serine 139 before and after SC35 depletion, and we detected DNA damage-induced foci in *SC35*-depleted MEFs (Fig. 5F). A similar result was also obtained with *ASF*/*SF2*-depleted MEFs (data not shown). DNA damage-induced foci were not observed in wt MEFs treated with Dox (data not shown). Together, these results suggest a critical role for SR proteins in maintaining genomic stability in vertebrates.

SC35-mediated cell proliferation is dependent on p53. The essential function of SC35 in cell proliferation in cell and animal models raised the possibility that SC35 is required for cell cycle progression of all proliferating cells. To test this hypothesis, we used siRNA to knock down SC35 in tumorigenic HCT116 colorectal carcinoma cells (Fig. 6A). While nonspecific control siRNA and specific siRNA against *U2AF65* had no detectable effect on cell proliferation on the basis of BrdU labeling, siRNA against *SC35* impaired cell proliferation in those cells. These results suggest a general requirement for SC35 in cell proliferation.

Because DNA damage is known to activate p53, and more importantly, because activated p53 has been shown to be essential for cell cycle arrest and apoptosis in response to DNA damage (6, 44), we asked whether p53 was required for *SC35*-dependent cell cycle progression. For this purpose, we took advantage of an isogenic HCT116 cell line in which *p53* was inactivated by homologous recombination (6). Strikingly, we found that *p53* inactivation was able to partially bypass the cell

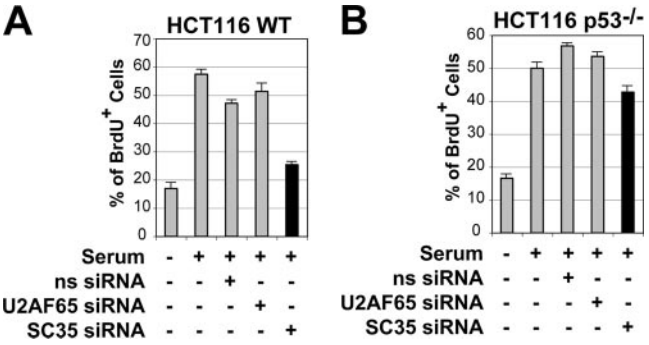

FIG. 6. SC35 is required for p53-dependent cell proliferation. (A and B) Microinjection of siRNA against SC35 and U2AF65 in wt HCT116 (A) and HCT116p53$^{-/-}$ (B) colon rectal carcinoma cells. A nonspecific (ns) siRNA was also microinjected as a control. Cell proliferation was analyzed by BrdU labeling.

cycle block (Fig. 6B). This observation prompted us to examine whether deletion of *p53* in vivo could rescue the *SC35* early embryonic-lethal phenotype. We crossed the SC35-heterozygous mice with p53-null mice. Mice with the *p53*$^{-/-}$/*SC35*$^{+/-}$ phenotype were obtained at the expected Mendelian frequency, but *p53*$^{-/-}$/*SC35*$^{-/-}$ embryos died at early gestation stages, indicating that the p53 pathway is only part of the *SC35*-dependent program in development (J.-H. Ding and X.-D. Fu, unpublished results). Therefore, SC35 may regulate cell proliferation in certain cell types in a *p53*-dependent manner, but the overall requirement for SC35 in animal development clearly involves both *p53*-dependent and -independent pathways.

Mechanisms of p53 activation in response to SC35 depletion. The p53 network is essential for a variety of stress-induced cellular responses, including cell cycle arrest, senescence, and apoptosis. To gain insights into the *p53*-dependent and *SC35*-mediated cell cycle arrest, we analyzed the expression profile of 96 key genes involved in the p53 pathway by using a commercially available mouse SuperArray (Fig. 7A). As predicted, a number of p53 target genes were significantly upregulated, including *Cdkn1a* (*p21*^{cip1}). By Western blot analysis, we confirmed that the level of p21^{cip1} protein was indeed dramatically elevated in *SC35*-depleted MEFs (Fig. 7B). We also observed induction of another cyclin-dependent kinase inhibitor, *p27*^{kip1}, a well-characterized target for the retinoblastoma protein (Fig. 7B). These findings suggest that SC35 depletion may have triggered multiple pathways to inhibit cell cycle progression.

The SuperArray profile also revealed upregulation of several p53 modifiers, including p300 acetyltransferase, Chek1 kinase, and Csnk2β kinase (Fig. 7A). This observation suggests that p53 may be activated in *SC35*-deficient MEFs by some specific posttranslational modification event(s). To determine the activation mechanisms, we examined the expression of p53 and its posttranslational modifications (Fig. 7C). While the overall p53 protein level for *SC35*-deficient MEFs was similar to that of wt MEFs, we found that phosphorylation at serine 18 was elevated, which was somewhat expected, because serine 18 is the major site for phosphorylation by activated ATM in response to double-strand DNA breaks (1, 3, 7, 36, 40), which were abundantly observed in *SC35*-depleted MEFs (Fig. 7C). Interestingly, besides p53 hyperphosphorylation, we also found

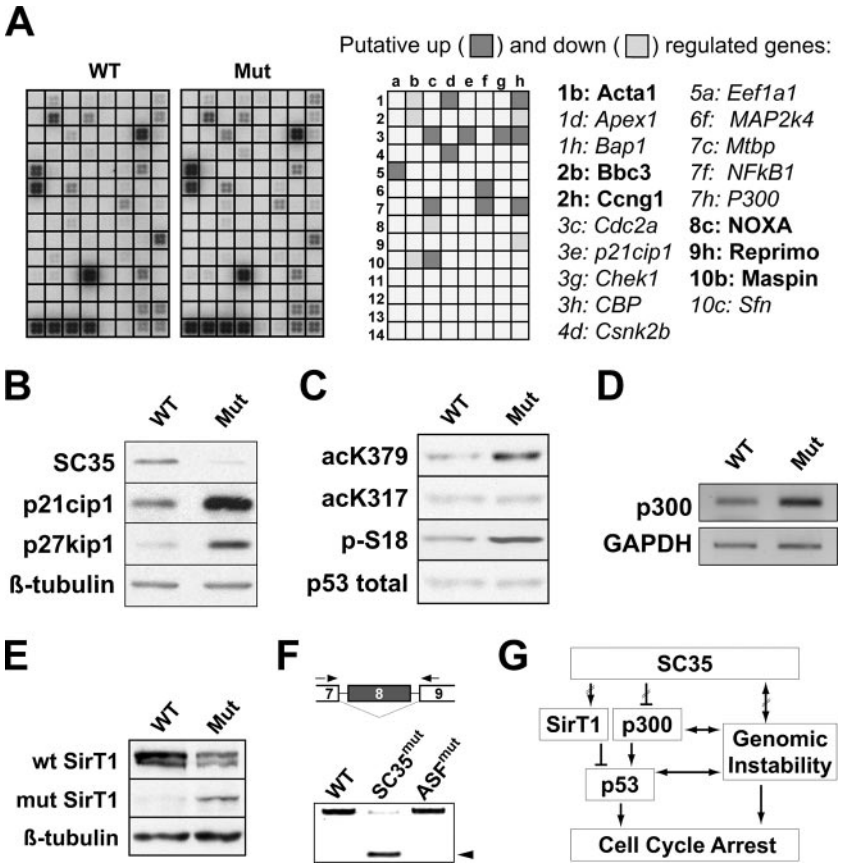

FIG. 7. Analyses of the p53 pathway in SC35-depleted MEFs. (A) Autoradiography of the p53 pathway gene expression levels using a SuperArray. WT, wild-type control MEFs; Mut, SC35-negative MEFs; Chk1, Chek1 kinase; CK2β, Csnk2β kinase. A schematic representation of the SuperArray results is presented at the right. Putative upregulated (italic) and downregulated (boldface) genes are listed. (B) Western blot analysis of the cyclin-dependent protein kinase inhibitors $p21^{cip1}$ and $p27^{kip1}$. (C) Western blot analysis of p53 posttranslational modifications using the indicated specific anti-p53 antibodies. p-S18, phosphorylation at serine 18; acK379, p53 hyperacetylation at lysine 379; acK317, p53 hyperacetylation at lysine 317. (D) Confirmation of induced p300 expression in SC35-depleted MEFs by RT-PCR. GAPDH, glyceraldehyde-3-phosphate dehydrogenase. (E) *SirT1* downregulation and identification of an aberrant form of SirT1 in SC35-depleted MEFs by Western blotting. (F) RT-PCR analysis of *SirT1* alternative splicing (arrowhead) using a pair of specific primers around exon 8 (arrows) in the SC35-depleted MEFs but not in the ASF/SF2-depleted MEFs. (G) Proposed mechanisms of SC35 regulation of cell cycle progression. Mut, the absence of SC35 after 5 days of Dox treatment.

p53 hyperacetylation at lysine 379 (Fig. 7C). This posttranslational event is consistent with the increased expression of p300 (Fig. 7A and D), which has been shown to act as a specific acetyltransferase towards the lysine 379 residue (4, 18, 23, 33, 39).

As p53 acetylation is regulated by both acetyltransferases and deacetylases, we further characterized this hyperacetylation event by examining the p53 deacetylase gene *SirT1* (2, 9, 34, 45), and we detected a significant reduction in the level of full-length SirT1 protein compared to that of wt control cells, along with a concurrent appearance of a truncated protein form in *SC35*-depleted MEFs (Fig. 7E). This observation raised the possibility that *SC35* depletion induced alternative splicing of the *SirT1* transcript. Reverse transcription-PCR (RT-PCR) analyses indeed confirmed this, revealing a smaller *SirT1* transcript, and direct sequencing of this PCR product showed specific skipping of exon 8 from the primary *SirT1* transcript (Fig. 7F). This particular alternative splicing event appears to be specific to *SC35* depletion in vivo, because a parallel analysis of *ASF*/*SF2* depletion in MEFs did not have the same effect on *SirT1* splicing (Fig. 7F). Therefore, different SR proteins may be required for cell cycle progression by affecting both common (e.g., activated ATM) and distinct (e.g., altered *SirT1* splicing) pathways. In the case of SC35, p53 hyperacetylation in conjunction with double-strand DNA break-induced p53 hyperphosphorylation may constitute some key events that lead to the observed cell cycle arrest (Fig. 7G).

DISCUSSION

The members of the SR family of splicing factors have been extensively studied at the level of biochemistry for their diverse roles in RNA metabolism and gene expression (20). However, few studies have linked their activities to specific pathways to elucidate their biological functions in vivo because of the lethal phenotype observed at the cellular and animal levels. Loss of a specific SR protein may be sufficient to induce some general effects that ultimately cause cell mortality. Li and Manley recently established such a general cellular response to SR protein deficiency, demonstrating a remarkable genomic instabil-

ity phenotype induced by DNA damage, and they linked the phenotype to a specific defect in the so-called R loop in ASF/*SF2*-deficient chicken DT40 cells (24, 26). We observed similar DNA damage events in normal diploid MEFs depleted of both SC35 and ASF/SF2, thus establishing the generality of the DNA damage-induced phenotype in vertebrates. Importantly, we observed that the DNA damage was not sufficient to prevent cell cycle progression through the S phase, despite the increased expression of $p21^{cip1}$ and $p27^{kip1}$. Instead, *SC35*-depleted MEFs were arrested in the G_2/M phase, apparently as a result of the activation of some major cell cycle regulators, such as $p21^{cip1}$ and $p27^{kip1}$.

The functional link between SC35 and cell cycle control is fully consistent with the essential function of SC35 in proliferating thymus (46) and pituitary (present study), but it is not an essential requirement in terminal differentiated mature cardiomyocytes (11). It is interesting that induced deletion of SC35 in matured hearts did not cause cardiac hypertrophy, which is in contrast to our earlier finding that SC35 deficiency in developing embryos triggered a later onset of cardiac hypertrophy in adult mice. As it is well known that a reduction in cell numbers during cardiogenesis can cause cardiac hypertrophy in adults, this result strongly supports the role of SC35 in cell proliferation in developing embryos, and a minor reduction in cell numbers manifests as a major functional consequence on adult life in response to an increased workload. Thus, the present data are consistent with and extend the earlier observation of the role of SC35 in developing hearts (11). The requirement for SC35 contrasts with the central role of ASF/SF2 in adult cardiomyocytes, suggesting an additional and unique requirement for this SR protein in heart performance, as we recently demonstrated during a physiological analysis of *ASF*/*SF2*-deficient hearts (48).

It has been shown that ASF/SF2 ablation in DT40 cells triggers apoptosis (29). Activation of the apoptotic pathway, however, may be specific for lymphocytes and other cell types but not for the developing heart and pituitary, as documented in a previous study (11) as well as the present study. Furthermore, we did not see any sign of programmed cell death in MEFs depleted of SC35 or ASF/SF2. Consistent with the activation of the DNA damage-responsive pathway, we found hyperphosphorylation of p53 at serine 18, a major site responsive to activation of the ATM pathway (1, 3, 7, 36, 40). Interestingly, in addition to the phosphorylation event induced by depletion of both SC35 and ASF/SF2, we detected a p53 hyperacetylation event that was uniquely triggered by depletion of SC35. The activation of the acetyltransferase gene *p300*, coupled with the downregulation of the *p53*-specific deacetylase gene *SirT1*, provided a plausible explanation for the observed p53 hyperacetylation event. It is less likely that the alternative splicing of *SirT1* alone is sufficient to cause p53 hyperacetylation, because we could not rescue the *SC35* mutant phenotypes with the full-length *SirT1*, and we could not mimic the SC35 phenotype by overexpressing the alternatively spliced version of *SirT1* (data not shown). These observations are consistent with the previous finding that genetic deletion of *SirT1* alone has a minimal effect on the level of p53 acetylation, and only upon the induction of genomic damage did *SirT1* mutant cells display p53 hyperacetylation (9, 45). Our observations are therefore fully consistent with those of the existing literature. Together, our results support the model that *SC35* deletion resulted in multiple molecular defects, including *SirT1* splicing, *p300* expression, and genomic instability, which in combination control cell proliferation (Fig. 7G).

The combined effect of p53 hyperphosphorylation and hyperacetylation may directly and potently regulate its downstream targets, including $p21^{cip1}$, to induce cell cycle arrest. Because we also observed the upregulation of $p27^{kip1}$, it is likely that SC35 also induces other cell cycle regulators besides those involved in the p53 pathway. Despite potential contributions by other pathways, however, we found that inactivation of p53 was able to partially relieve the cell cycle block in HCT116 colon carcinoma cells, suggesting that activated p53 is functionally responsible, at least in part, for the observed cell cycle arrest induced by *SC35* depletion. However, it is also clear that the activation of the p53 pathway is insufficient to account for the full spectrum of SC35 functions in vivo, because the *SC35*-null mutation in the *p53*-null background still causes embryonic lethality (J.-H. Ding and X.-D. Fu, unpublished). Likewise, it has been shown that overcoming genomic instability induced by *ASF*/*SF2* depletion is insufficient to prevent cell death in chicken DT40 cells (26). Together, these observations suggest that SR proteins contribute to multiple critical pathways in the regulation of cell proliferation.

The involvement of SC35, and likely other SR proteins, in some major regulatory pathways for cell proliferation and cell cycle progression is fully corroborated by increasing evidence that the SR family of splicing factors and regulators may directly contribute to the oncogenic process. Indeed, elevated levels of expression of SR proteins has been detected in multiple types of tumors (13, 16, 43, 49). In most cases, however, their exact roles in tumorigenesis are unknown, although two recent studies suggest a specific role of ASF/SF2 in tumorigenesis. ASF/SF2 appears to be specifically involved in regulated splicing of the Ron proto-oncogene, and the splicing defect appears to directly contribute to elevated cellular motility and invasiveness (15). More recently, overexpression of ASF/SF2 was found to induce cell transformation due to altered splicing of the p70S6 kinase, a key effector downstream of the mTOR (mammalian target of rapamycin) pathway (19, 22). Thus, this and other specific regulatory events may play an important part in tumor progression in vivo. Furthermore, the ability of SR proteins to affect genomic stability and integrity may provide a mechanism to facilitate tumor development, selection, and expansion. Here, we have shown that SR proteins are involved in the regulation of the p53 pathway, which is a well-known tumor suppressor gene. Since ablation of specific SR proteins can activate p53, it is conceivable that overexpression of SC35 and other SR proteins in tumors directly or indirectly suppresses p53 in addition to modulating other critical cellular genes at the level of splicing, which together may enhance cell proliferation in a misregulated fashion.

ACKNOWLEDGMENTS

We are grateful to J. Zhang and X. Xu for advice and technical assistance during the course of the study and L. E. Olsen for providing the *Pitx*/*Cre* transgenic mice.

This study was supported by grants from the NIH to M.G.R. and X.-D.F. and by an NIDDK Research Career Award to X.L. M.G.R is an investigator of the Howard Hughes Medical Institute. X.L. is a Basil

O'Connor scholar and the recipient of an award from the Charles H. Hood Foundation, Inc., Boston, MA.

REFERENCES

1. **Abraham, R. T.** 2001. Cell cycle checkpoint signaling through the ATM and ATR kinases. Genes Dev. **15:**2177–2196.
2. **Avalos, J. L., I. Celic, S. Muhammad, M. S. Cosgrove, J. D. Boeke, and C. Wolberger.** 2002. Structure of a Sir2 enzyme bound to an acetylated p53 peptide. Mol. Cell **10:**523–535.
3. **Banin, S., L. Moyal, S. Shieh, Y. Taya, C. W. Anderson, L. Chessa, N. I. Smorodinsky, C. Prives, Y. Reiss, Y. Shiloh, and Y. Ziv.** 1998. Enhanced phosphorylation of p53 by ATM in response to DNA damage. Science **281:**1674–1677.
4. **Barlev, N. A., L. Liu, N. H. Chehab, K. Mansfield, K. G. Harris, T. D. Halazonetis, and S. L. Berger.** 2001. Acetylation of p53 activates transcription through recruitment of coactivators/histone acetyltransferases. Mol. Cell **8:**1243–1254.
5. **Black, D. L.** 2000. Protein diversity from alternative splicing: a challenge for bioinformatics and post-genome biology. Cell **103:**367–370.
6. **Bunz, F., A. Dutriaux, C. Lengauer, T. Waldman, S. Zhou, J. P. Brown, J. M. Sedivy, K. W. Kinzler, and B. Vogelstein.** 1998. Requirement for p53 and p21 to sustain G_2 arrest after DNA damage. Science **282:**1497–1501.
7. **Canman, C. E., D. S. Lim, K. A. Cimprich, Y. Taya, K. Tamai, K. Sakaguchi, E. Appella, M. B. Kastan, and J. D. Siliciano.** 1998. Activation of the ATM kinase by ionizing radiation and phosphorylation of p53. Science **281:**1677–1679.
8. **Cazalla, D., J. Zhu, L. Manche, E. Huber, A. R. Krainer, and J. F. Caceres.** 2002. Nuclear export and retention signals in the RS domain of SR proteins. Mol. Cell. Biol. **22:**6871–6882.
9. **Cheng, H. L., R. Mostoslavsky, S. Saito, J. P. Manis, Y. Gu, P. Patel, R. Bronson, E. Appella, F. W. Alt, and K. F. Chua.** 2003. Developmental defects and p53 hyperacetylation in Sir2 homolog (SIRT1)-deficient mice. Proc. Natl. Acad. Sci. USA **100:**10794–10799.
10. **Dasen, J. S., S. M. O'Connell, S. E. Flynn, M. Treier, A. S. Gleiberman, D. P. Szeto, F. Hooshmand, A. K. Aggarwal, and M. G. Rosenfeld.** 1999. Reciprocal interactions of Pit1 and GATA2 mediate signaling gradient-induced determination of pituitary cell types. Cell **97:**587–598.
11. **Ding, J. H., X. Xu, D. Yang, P. H. Chu, N. D. Dalton, Z. Ye, J. M. Yeakley, H. Cheng, R. P. Xiao, J. Ross, et al.** 2004. Dilated cardiomyopathy caused by tissue-specific ablation of SC35 in the heart. EMBO J. **23:**885–896.
12. **Faustino, N. A., and T. A. Cooper.** 2003. Pre-mRNA splicing and human disease. Genes Dev. **17:**419–437.
13. **Fischer, D. C., K. Noack, I. B. Runnebaum, D. O. Watermann, D. G. Kieback, S. Stamm, and E. Stickeler.** 2004. Expression of splicing factors in human ovarian cancer. Oncol. Rep. **11:**1085–1090.
14. **Fu, X. D.** 1995. The superfamily of arginine/serine-rich splicing factors. RNA **1:**663–680.
15. **Ghigna, C., S. Giordano, H. Shen, F. Benvenuto, F. Castiglioni, P. M. Comoglio, M. R. Green, S. Riva, and G. Biamonti.** 2005. Cell motility is controlled by SF2/ASF through alternative splicing of the Ron protooncogene. Mol. Cell **20:**881–890.
16. **Ghigna, C., M. Moroni, C. Porta, S. Riva, and G. Biamonti.** 1998. Altered expression of heterogenous nuclear ribonucleoproteins and SR factors in human colon adenocarcinomas. Cancer Res. **58:**5818–5824.
17. **Graveley, B. R.** 2000. Sorting out the complexity of SR protein functions. RNA **6:**1197–1211.
18. **Gu, W., and R. G. Roeder.** 1997. Activation of p53 sequence-specific DNA binding by acetylation of the p53 C-terminal domain. Cell **90:**595–606.
19. **Hu, A., and X.-D. Fu.** 2007. Splicing oncogenes. Nat. Struct. Mol. Biol. **14:**174–175.
20. **Huang, Y., and J. A. Steitz.** 2005. SRprises along a messenger's journey. Mol. Cell **17:**613–615.
21. **Jumaa, H., G. Wei, and P. J. Nielsen.** 1999. Blastocyst formation is blocked in mouse embryos lacking the splicing factor SRp20. Curr. Biol. **9:**899–902.
22. **Karni, R., E. de Stanchina, S. W. Lowe, R. Sinha, D. Mu, and A. R. Krainer.** 2007. The gene encoding the splicing factor SF2/ASF is a proto-oncogene. Nat. Struct. Mol. Biol. **14:**185–193.
23. **Krummel, K. A., C. J. Lee, F. Toledo, and G. M. Wahl.** 2005. The C-terminal lysines fine-tune P53 stress responses in a mouse model but are not required for stability control or transactivation. Proc. Natl. Acad. Sci. USA **102:**10188–10193.
24. **Li, X., and J. L. Manley.** 2006. Cotranscriptional processes and their influence on genome stability. Genes Dev. **20:**1838–1847.
25. **Li, X., and T. Lufkin.** 2000. Cre recombinase expression in the floorplate, notochord and gut epithelium in transgenic embryos driven by the Hoxa-1 enhancer III. Genesis **26:**121–122.
26. **Li, X., and J. L. Manley.** 2005. Inactivation of the SR protein splicing factor ASF/SF2 results in genomic instability. Cell **122:**365–378.
27. **Li, X., and J. L. Manley.** 2006. Alternative splicing and control of apoptotic DNA fragmentation. Cell Cycle **5:**1886–1901.
28. **Li, X., V. Perissi, F. Liu, D. W. Rose, and M. G. Rosenfeld.** 2002. Tissue-specific regulation of retinal and pituitary precursor cell proliferation. Science **297:**1180–1183.
29. **Li, X., J. Wang, and J. L. Manley.** 2005. Loss of splicing factor ASF/SF2 induces G_2 cell cycle arrest and apoptosis but inhibits internucleosomal DNA fragmentation. Genes Dev. **19:**2705–2714.
30. **Li, X., W. Wang, and T. Lufkin.** 1997. Dicistronic LacZ and alkaline phosphatase reporter constructs permit simultaneous histological analysis of expression from multiple transgenes. BioTechniques **23:**874–882.
31. **Lin, S., and X.-D. Fu.** 2007. SR proteins and related factors in alternative splicing. *In* B. Blencowe and B. Graveley (ed.), Alternative splicing in the postgenomic era. Eurekah Bioscience Series. Landes Bioscience, Austin, TX.
32. **Lin, S., R. Xiao, P. Sun, X. Xu, and X. D. Fu.** 2005. Dephosphorylation-dependent sorting of SR splicing factors during mRNP maturation. Mol. Cell **20:**413–425.
33. **Liu, L., D. M. Scolnick, R. C. Trievel, H. B. Zhang, R. Marmorstein, T. D. Halazonetis, and S. L. Berger.** 1999. p53 sites acetylated in vitro by PCAF and p300 are acetylated in vivo in response to DNA damage. Mol. Cell. Biol. **19:**1202–1209.
34. **Luo, J., A. Y. Nikolaev, S. Imai, D. Chen, F. Su, A. Shiloh, L. Guarente, and W. Gu.** 2001. Negative control of p53 by Sir2α promotes cell survival under stress. Cell **107:**137–148.
35. **Manley, J. L., and R. Tacke.** 1996. SR proteins and splicing control. Genes Dev. **10:**1569–1579.
36. **Nakagawa, K., Y. Taya, K. Tamai, and M. Yamaizumi.** 1999. Requirement of ATM in phosphorylation of the human p53 protein at serine 15 following DNA double-strand breaks. Mol. Cell. Biol. **19:**2828–2834.
37. **Olson, L. E., J. Tollkuhn, C. Scafoglio, A. Krones, J. Zhang, K. A. Ohgi, W. Wu, M. M. Taketo, R. Kemler, R. Grosschedl, et al.** 2006. Homeodomain-mediated beta-catenin-dependent switching events dictate cell-lineage determination. Cell **125:**593–605.
38. **Rhodes, S. J., R. Chen, G. E. DiMattia, K. M. Scully, K. A. Kalla, S. C. Lin, V. C. Yu, and M. G. Rosenfeld.** 1993. A tissue-specific enhancer confers Pit-1-dependent morphogen inducibility and autoregulation on the *pit-1* gene. Genes Dev. **7:**913–932.
39. **Sakaguchi, K., J. E. Herrera, S. Saito, T. Miki, M. Bustin, A. Vassilev, C. W. Anderson, and E. Appella.** 1998. DNA damage activates p53 through a phosphorylation-acetylation cascade. Genes Dev. **12:**2831–2841.
40. **Shiloh, Y.** 2003. ATM and related protein kinases: safeguarding genome integrity. Nat. Rev. Cancer **3:**155–168.
41. **Sohal, D. S., M. Nghiem, M. A. Crackower, S. A. Witt, T. R. Kimball, K. M. Tymitz, J. M. Penninger, and J. D. Molkentin.** 2001. Temporally regulated and tissue-specific gene manipulations in the adult and embryonic heart using a tamoxifen-inducible Cre protein. Circ. Res. **89:**20–25.
42. **Soriano, P.** 1999. Generalized *lacZ* expression with the ROSA26 Cre reporter strain. Nat. Genet. **21:**70–71.
43. **Stickeler, E., F. Kittrell, D. Medina, and S. M. Berget.** 1999. Stage-specific changes in SR splicing factors and alternative splicing in mammary tumorigenesis. Oncogene **18:**3574–3582.
44. **Taylor, W. R., and G. R. Stark.** 2001. Regulation of the G_2/M transition by p53. Oncogene **20:**1803–1815.
45. **Vaziri, H., S. K. Dessain, E. Ng Eaton, S. I. Imai, R. A. Frye, T. K. Pandita, L. Guarente, and R. A. Weinberg.** 2001. hSIR2(SIRT1) functions as an NAD-dependent p53 deacetylase. Cell **107:**149–159.
46. **Wang, H. Y., X. Xu, J. H. Ding, J. R. Bermingham, Jr., and X. D. Fu.** 2001. SC35 plays a role in T cell development and alternative splicing of CD45. Mol. Cell **7:**331–342.
47. **Wang, J., Y. Takagaki, and J. L. Manley.** 1996. Targeted disruption of an essential vertebrate gene: ASF/SF2 is required for cell viability. Genes Dev. **10:**2588–2599.
48. **Xu, X., D. Yang, J. H. Ding, W. Wang, P. H. Chu, N. D. Dalton, H. Y. Wang, J. R. Bermingham, Jr., Z. Ye, F. Liu., et al.** 2005. ASF/SF2-regulated CaMKIIΔ alternative splicing temporally reprograms excitation-contraction coupling in cardiac muscle. Cell **120:**59–72.
49. **Zerbe, L. K., I. Pino, R. Pio, P. F. Cosper, L. D. Dwyer-Nield, A. M. Meyer, J. D. Port, L. M. Montuenga, and M. A. Malkinson.** 2004. Relative amounts of antagonistic splicing factors, hnRNP A1 and ASF/SF2, change during neoplastic lung growth: implications for pre-mRNA processing. Mol. Carcinog. **41:**187–196.